

- mechanism involving A⁻.
20. M. L. Bender *et al.*, *J. Am. Chem. Soc.* **86**, 3680 (1964); A. Himoe and G. P. Hess, *Biochem. Biophys. Res. Commun.* **23**, 234 (1966).
 21. S. Sprang *et al.*, *Science* **237**, 905 (1987).
 22. R. Henderson, *Biochem. J.* **124**, 13 (1971); J. Fastrez and N. Houyet, *Eur. J. Biochem.* **81**, 515 (1977).
 23. C. D. Hubbard and J. F. Kirsch, *Biochemistry* **11**, 2483 (1972).
 24. R. Kitz and F. S. Wilson, *J. Biol. Chem.* **237**, 3245 (1962).
 25. Incubations with diisopropylfluorophosphate (DFP) were performed at 25°C with 100 nM wild-type or mutant enzyme and varying concentrations of DFP in either 50 mM Taps (3-[[tris(hydroxymethyl)methyl]amino]propanesulfonic acid), pH 7.96, or 50 mM glycine, pH 10.03, that contained 0.1M NaCl, 1 mM CaCl₂, 0.005% (w/v) Triton X-100 and 5% (v/v) isopropanol. DFP stock solutions were made up in isopropanol. Final volumes were 0.200 ml and 6.2 ml when incubations were performed with trypsin and D 102 N trypsin, respectively. Trypsin enzyme activities were measured spectrophotometrically at 324 nm by adding 10 µl of the trypsin-DFP solution to 0.99 ml of the same buffer (1 nM trypsin final concentration) that contained 60 µM *N*-benzyloxycarbonyl-L-lysine benzylthioester (Z-Lys-S-Bzl) and 250 µM 4,4'-dithiodipyridine but no DFP. Mutant enzyme activities at 324 nm were determined by adding 10 µl of 6 mM Z-Lys-S-Bzl and 10 µl of 25 mM 4,4'-dithiodipyridine to 0.98 ml of the D 102 N trypsin-DFP solution. The concentrations of DFP during incubations with trypsin at both pH values were 0, 20, 25, 40, 80, or 200 µM. In incubations with D 102 N trypsin initial DFP concentrations were 0, 5, 8, 10, or 12.5 mM, and 0, 10, 12.5, or 16.6 mM when assays were performed at pH 7.96 and pH 10.03, respectively.
 26. T. Yosigimura, L. N. Barker, J. C. Powers, *J. Biol. Chem.* **257**, 5077 (1982).
 27. Incubations with tosyl-L-lysine chloromethyl ketone (TLCK) were performed at 25°C with 5 µM unmodified or mutant enzyme in 100 µl of either 100 mM Mops [3-*N*(morpholino)propanesulfonic acid], pH 7.16 or 100 mM Taps, pH 8.77, that contained either 0 or 200 µM TLCK. Immediately before assaying trypsin activity an aliquot from the incubation mixtures was diluted 20-fold in 50 mM incubation buffer that contained 0.1M NaCl, 1 mM CaCl₂, and 0.005% (w/v) Triton X-100. Ten microliters of the diluted enzyme solution was added to 0.99 ml of the dilution buffer that contained 250 µM 4,4'-dithiodipyridine and 100 µM Z-Lys-S-Bzl (assay buffer); enzyme activities were followed at 25°C spectrophotometrically at 324 nm (2.5 nM trypsin). Mutant enzyme activities were determined in an identical manner as described above except that 10 µl of the incubation mixture that contained D 102 N trypsin was added directly to 0.99 ml of the assay buffer (50 nM D 102 N trypsin). After 3 hours of incubation with TLCK the loss of catalytic activity of both enzymes at both pH values was complete. Since there was no activity of either enzyme after 2.5 hours of further incubation with a large excess of substrate over TLCK, the inhibition was probably due to formation of a covalent bond between the enzyme and the inhibitor and not to a slow-off rate for a noncovalently bound competitive inhibitor.
 28. F. J. Kezdy and M. L. Bender, *Biochemistry* **1**, 1097 (1962).
 29. Substrate concentrations were calculated by using the total change in absorbance at 324 nm when reactions were run at pH 7.5 [$\epsilon_{324} = 19,800 M^{-1} cm^{-1}$ (13)] and catalyzed by 1 nM trypsin so that the reaction would be completed within several minutes. The molar absorptivities over the pH range of 4.1 to 10.6 were determined by repeating these reactions with known substrate concentrations at various pH values. It was found that at pH values below 7.6 the molar absorptivity remained at $19,800 M^{-1} cm^{-1}$, but that this value decreased sigmoidally above pH 7.6, with an apparent pK_a of 8.7, presumably reflecting the ionization of thiopyridine. These molar absorptivity values were used to convert rates of reaction into molar rates at the appropriate pH values.

The concentration of viable active sites in native enzyme preparations were determined by active site titrations with 4-methylumbelliferyl *p*-guanidinobenzoate (MUGB) by using 4-methylumbelliferone as a standard (30) as described in the legend to Table 1. Titrations of D 102 N trypsin proved to be too slow to measure active sites accurately. Mutant enzyme concentrations were thus determined in duplicate by absorbance at 280 nm ($\epsilon_{280} = 38,000 M^{-1} cm^{-1}$). The accuracy of this molar absorptivity value was confirmed by amino acid analysis with norleucine as an internal standard.

A danger in following the activity of D 102 N trypsin is that an unknown proportion of the activity may be due to trypsin that has formed through deamidation. This does not appear to be a problem at pH values less than 8 where the activity of the mutant enzyme is less than 0.1% that of trypsin. At alkaline pH values, where the activity of the mutant enzyme becomes significant, the possibility of activity resulting from deamidation becomes greater. However, assays with 100 nM D 102 N trypsin and

60 µM Z-Lys-S-Bzl as substrate at pH 7.16 and pH 10.24 after prior incubation of the enzyme in buffers at either pH value for 1 hour gave initial rates of reaction of $1.00 \pm 0.04 min^{-1}$ and $249 \pm 5 min^{-1}$, respectively. These results indicate that significant deamidation of the D 102 N residue to an aspartic acid did not occur in the pH and time ranges studied.

30. G. W. Jameson, D. V. Roberts, R. W. Adams, S. A. Kyle, D. T. Elmore, *Biochem. J.* **131**, 107 (1973).
31. D. V. Roberts, in *Enzyme Kinetics* (Cambridge Univ. Press, Cambridge, 1977), p. 299.
32. K. Yamaoka *et al.*, *J. Pharm. Dyn.* **4**, 879 (1981).
33. We thank J. F. Kirsch and E. T. Kaiser for helpful discussions and L. Spector for preparing the manuscript. Support by NSF grant PCM830610 (W.J.R.) and DMB8608086 (C.S.C.), and a Bristol Meyer grant of Research Corporation (C.S.C.) is gratefully acknowledged. An NIH postdoctoral fellowship was awarded to S.R. (GM 10765).

29 September 1986; accepted 29 May 1987

Adrenal Medulla Grafts Enhance Recovery of Striatal Dopaminergic Fibers

MARTHA C. BOHN,* LISA CUPIT, FREDERICK MARCIANO, DON M. GASH

The drug, 1-methyl-4-phenyl-1,2,5,6-tetrahydropyridine (MPTP), depletes striatal dopamine levels in primates and certain rodents, including mice, and produces parkinsonian-like symptoms in humans and nonhuman primates. To investigate the consequences of grafting adrenal medullary tissue into the brain of a rodent model of Parkinson's disease, a piece of adult mouse adrenal medulla was grafted unilaterally into mouse striatum 1 week after MPTP treatment. This MPTP treatment resulted in the virtual disappearance of tyrosine hydroxylase-immunoreactive fibers and severely depleted striatal dopamine levels. At 2, 4, and 6 weeks after grafting, dense tyrosine hydroxylase-immunoreactive fibers were observed in the grafted striatum, while only sparse fibers were seen in the contralateral striatum. In all cases, tyrosine hydroxylase-immunoreactive fibers appeared to be from the host rather than from the grafts, which survived poorly. These observations suggest that, in mice, adrenal medullary grafts exert a neurotrophic action in the host brain to enhance recovery of dopaminergic neurons. This effect may be relevant to the symptomatic recovery in Parkinson's disease patients who have received adrenal medullary grafts.

IN HUMANS, THE DRUG, 1-METHYL-4-PHENYL-1,2,5,6-TETRAHYDROPYRIDINE (MPTP), produces motor deficits that closely resemble those observed in Parkinson's disease (1-4). This observation has led to the development of animal models of Parkinson's disease that are valuable for studying the effects of brain grafting (5). MPTP damages the dopamine (DA)-containing A9 cell group in the pars compacta of the substantia nigra and results in a degeneration of the nigrostriatal DA fibers and loss of striatal DA and its metabolites (1-8). The severity of this damage is species-dependent. In primates, MPTP treatment damages both the DA fibers and cell bodies (1-5). In mice, the fibers are damaged, but many A9 neurons survive (6, 7). Because the MPTP lesion is transient in mouse (7, 9), the MPTP-treated mouse provides an opportunity for studying recovery of identified neurons in the brain. Our study suggests

that striatal grafts of adult mouse adrenal medulla enhance recovery of these neurons.

Two MPTP treatments were compared for their effects on striatal DA levels and tyrosine hydroxylase-immunoreactivity (TH-IR) in the striatum and A9 region of C57BL/6 mice (6 to 12 weeks old; 21 to 28 g). As described (6, 7), lightly etherized mice received multiple injections of MPTP-HCl subcutaneously in 0.5 ml of saline. Group A received three injections of 30 mg per kilogram of body weight at 24-hour intervals and group B received two injections of 50 mg per kilogram of body weight 16 hours apart. Catecholamines in tissues were isolated and measured

M. C. Bohn and L. Cupit, Department of Neurobiology and Behavior, State University of New York, Stony Brook, NY 11794.
F. Marciano and D. M. Gash, Department of Neurobiology and Anatomy, University of Rochester School of Medicine, Rochester, NY 14642.

*To whom correspondence should be addressed.

Table 1. Effects of MPTP treatment on neostriatal TH-IR fibers and dopamine levels. For catecholamine determinations, mice were killed by decapitation and the neostriatum frozen in liquid nitrogen. Tissue was weighed frozen, homogenized by sonication in 10 volumes of 0.1N perchloric acid containing 0.025% EDTA and 15 ng of dihydroxybenzylamine as an internal standard, and centrifuged. Supernatant (50 μ l) was extracted with 50 mg of activated alumina in 1 ml 0.5M tris buffer, pH 8.6. After washing the alumina twice with 0.01M tris, pH 7.0, the catecholamines were eluted into 1 ml of 0.2N acetic acid. The filtered eluant was assayed on a Bioanalytical high-performance liquid chromatograph with an Altex Ultrasphere column equilibrated with 0.1M phosphate buffer, pH 3.0, containing 0.1 mM EDTA, 0.2 mM sodium octylsulfonate, 1% methanol, and 1.5% acetonitrile. Catecholamines were detected by electrochemical oxidation at a glassy carbon electrode (0.72 V) and quantified by comparison to the internal standard. Statistically significant differences were determined in the Newman-Keuls test after an analysis of variance. Dopamine amounts are expressed as mean \pm SEM.

Treatment	<i>n</i>	Survival (weeks)	Dopamine (ng/mg tissue)	Effect	TH-IR fibers
Normal	10	—	10.81 \pm 1.14	—	Dense
MPTP (group A)	6	2	0.50 \pm 0.14*	—95%	None
MPTP (group A)	8	5	8.73 \pm 1.06	NSD†	Dense
MPTP (group B)	8	5	1.50 \pm 0.24*	—86%	Sparse

**P* \leq 0.01 with respect to normal mice. †NSD, not significantly different.

as described (Table 1) (10). In group A, striatal DA levels were depleted to 5% of normal values 2 weeks after MPTP treatment. However, by 5 weeks, striatal DA levels were not significantly different from those in normal mice (Table 1). This recovery was paralleled by a reappearance of dense TH-IR fibers in the striatum. In contrast, in group B mice, striatal DA was chronically depleted to 14% of normal levels 5 weeks after MPTP treatment and only sparse fibers were observed (Table 1). In contrast to the central effects of MPTP, neither of the MPTP treatment schedules significantly affected adrenal catecholamine levels.

To investigate the fate of adult adrenal medullary tissue grafted into the brain parenchyma, group B mice received unilateral homografts of adrenal medulla from untreated mice 1 week after MPTP treatment. Young adult male C57BL/6 mice served as both tissue donors and recipients. To provide the donor tissue, lightly etherized mice were decapitated and the adrenals quickly removed. Under a dissecting microscope, the adrenals were bisected, and the adrenal medulla was dissected free from the cortex and maintained in cold sterile calcium- and magnesium-free buffer (11) until transplanted. The tissue recipients were anesthetized with 0.3 ml of chloropentane per 100 g of body weight (Fort Dodge, Indiana) and placed in a stereotaxic apparatus to stabilize the head. The skin was opened and an electric dental burr was used to expose the left cerebral cortex rostrolateral to bregma. A 25-gauge cannula was used to aspirate through the cortex and corpus callosum to expose the head of the caudate nucleus. Gelfoam was packed into the cavity for several minutes to control any bleeding, the Gelfoam was removed, and adrenal medullary fragments (approximately 0.2 to 0.5 mm in length) were inserted directly into

the striatum with a pair of fine forceps. The same piece of Gelfoam was inserted into the cortical cavity and the wound was closed. The time from the killing of the donor to implantation in the host averaged 30 minutes and was never longer than 2 hours. Control groups consisted of either MPTP-treated mice lacking a graft or MPTP-treated mice with sham surgery in which Gelfoam was inserted into the striatum. Grafted cells and the host striatum were examined at 2, 4, or 6 weeks after surgery (*n* = 4 to 5 per group).

Neurotransmitter phenotypic expression in grafted cells was studied by staining for immunoreactivity to enzymes in the catecholamine pathway—TH, the rate-limiting enzyme, and phenylethanolamine *N*-methyltransferase (PNMT), the epinephrine synthesizing enzyme. Although grafted cells survived in all mice, most of the grafted cells appeared to be dying, and the grafts were filled with autofluorescent material and macrophages. Some of the grafts (5 of 13) contained TH-IR cells. Although these TH-IR cells were rare, some had neuronal-like processes (Fig. 1A). However, none of these processes appeared to be growing out of the graft site. Three of these grafts and two others also contained clumps of PNMT-IR cells that had retained a chromaffin cell-like morphology (Fig. 1B).

Effects of the MPTP treatment and adrenal grafts on the nigrostriatal system in the host brain were also investigated by studying TH-IR. In both treatment groups, only sparse TH-IR fibers were observed in the dorsal striatum 2 weeks after the last MPTP injection. However, 5 weeks after MPTP administration, marked differences were seen between the two groups. Dense TH-IR fibers were observed in the striatum of group A mice, while only sparse fibers were observed in group B mice. In all MPTP-

treated mice, TH-IR neurons were present in the substantia nigra; however, the intensity of staining appeared to be less than in normal mice. Although the number of these neurons appeared reduced, this effect was not quantified because it has been previously reported (6).

The density of TH-IR fibers in the dorsal striatum in all mice receiving grafts showed marked recovery on the side of the graft at all survival times (Fig. 1D). In contrast, no recovery was observed at 6 weeks (*n* = 4) in mice that received sham grafts of Gelfoam. TH-IR fibers were especially dense near the graft, although they did not penetrate into the graft. Minimal recovery was observed on the contralateral side in graft recipients (Fig. 1C); however, in some mice, patches of TH-IR fibers were observed near the ventricle, suggesting a response to a diffusible factor that had limited access to the contralateral striatum. To determine whether the recovery of TH-IR fibers was due to a response of sympathetic noradrenergic fibers innervating blood vessels or noradrenergic fibers of central origin, sections were examined for immunoreactivity to dopamine β -hydroxylase (DBH). The striatal fibers lacked DBH-IR, suggesting that they were dopaminergic and not noradrenergic.

These observations suggest that grafts of adrenal medulla promote the recovery of MPTP-damaged dopaminergic neurons. Although the source of these fibers has not yet been identified, it is likely that they are from the A9 cell group because some of these neurons survived MPTP treatment. However, we have not excluded the possibility that other dopaminergic neurons that are relatively unaffected by MPTP treatment (12, 13) may have sprouted fibers into this region. In either case sprouting must have occurred, because the density of fibers in the grafted striatum exceeded that in the striatum of normal mice. It is assumed that MPTP treatment destroys the DA-containing fibers in the striatum, an assumption based on the loss of catecholamine synthesizing characters. A sprouting or regeneration of these "pruned" fibers could account for the reappearance of TH-IR fibers. An alternative explanation might be that the fibers of surviving cells did not degenerate, but were not detected due to a transient cessation of expression or transport of catecholamine enzymes. A biochemical recovery in MPTP damaged neurons could have rapidly restored these enzymes; however, this alone could not account for the apparent exuberance of fibers in the grafted striatum.

Grafted cells did not appear to contribute to the recovery in TH-IR fibers, since few TH-IR cells survived and only a small proportion of these had grown processes. Nev-

ertheless, grafted cells produced a profound effect on morphological recovery in the host brain. Several mechanisms could account for this recovery. (i) The adrenal graft may have released a neurotrophic factor that stimulated growth, cell survival, or catecholamine regulation in central DA neurons. Such a factor might be produced by the medullary cells or by non-neuronal cells such as Schwann cells included in the graft. (ii) The grafts may have stimulated gliosis, which in turn resulted in the production of a neurotrophic factor of glial origin. This possibility

is supported by studies suggesting that glial cells promote neuronal recovery in the brain (14, 15) and observations indicating that most neuronal growth factors are non-neuronal in origin (16). (iii) Recovery might have been promoted by a factor produced by macrophages entering the area to clean up the dying grafted cells or by changes in the blood-brain barrier (17). (iv) The graft itself or cellular reactions occurring after grafting may have acted as scavengers for 1-methyl-4-phenylpyridine, which is thought to be the active neurotoxin accounting for the

effects of MPTP treatment (18, 19). Such a protective effect would be similar to that of striatal grafts reducing the effects of kainic acid (20). Although our data cannot distinguish among these possible mechanisms, they support the concept that graft-induced recovery of neurodegeneration in the brain, whether caused by disease or injury, may occur through processes other than direct restoration of function by the grafted cells themselves (15, 20, 21). The graft may instead act as a mediator to promote the production of growth factors or growth mechanisms leading to plasticity and recovery of cells in the host.

These studies are of interest in view of similar studies in Sweden and Mexico that have used autografts of adrenal medulla to treat humans with Parkinson's disease (22, 23). In one of these studies, prolonged improvement in motor symptoms was reported to result from the grafts (23). Although this improvement might be due to DA produced by grafted cells or to innervation of host striatum by grafted cells, our study suggests that improvement might also be due to graft-induced recovery of DA neurons in the brain of patients with Parkinson's disease. This mechanism may also be involved in the behavioral recovery observed in nonhuman primate models of Parkinson's disease following fetal grafts of substantia nigra (5).

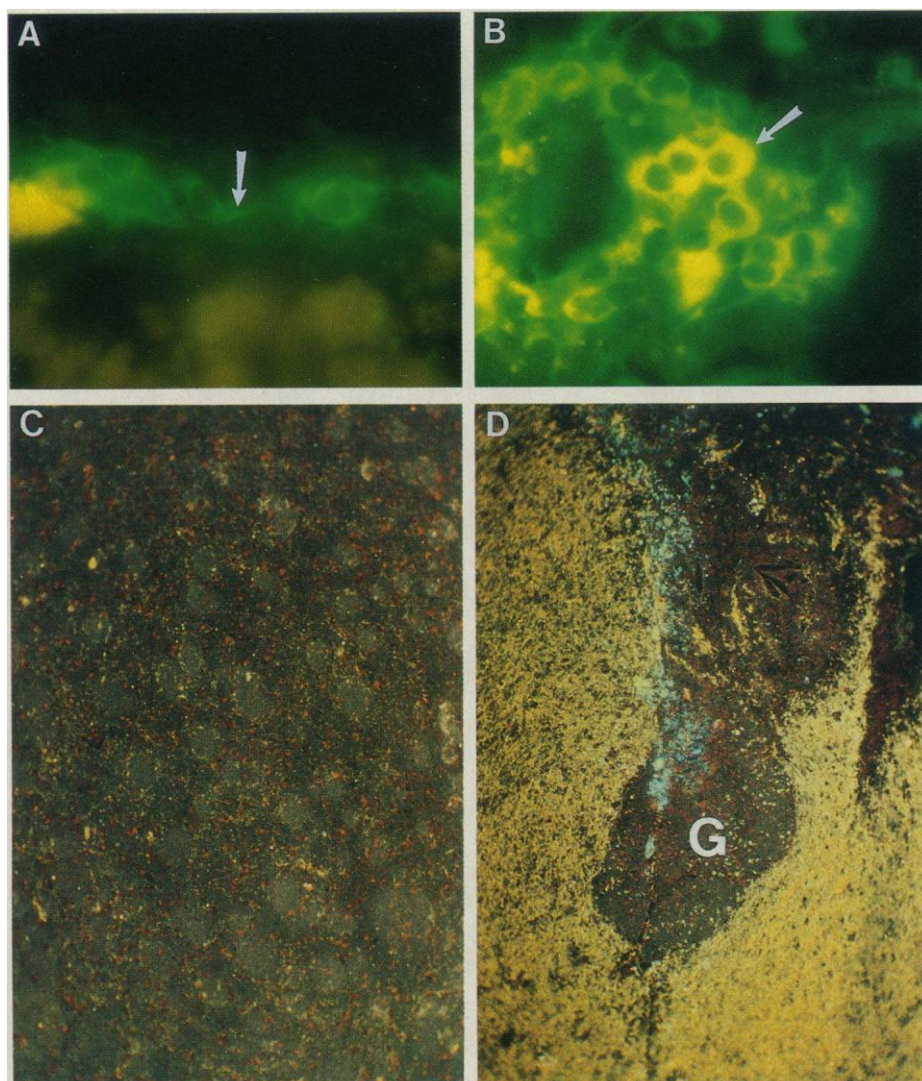


Fig. 1. Immunofluorescence of TH and PNMT in adrenal medulla grafts. (A) TH-IR cells (green) on the edge of the graft deep in the striatum. Note the cellular processes (arrow). Yellow material is autofluorescent lipofuscin in atrophic cells within graft. Magnification, $\times 720$. (B) PNMT-IR chromaffin-like cells (arrow) on the caudal surface of the graft. Magnification, $\times 550$. For both antigens, mice under ketamine-rompum anesthesia were perfused through the heart with saline, then with ice-cold 4% paraformaldehyde in 0.1M phosphate buffer, pH 7.4. Cryostat sections (15 μ m) were incubated overnight with rabbit antiserum to rat TH (1:1000; Eugene Tech) or rabbit antiserum to rat PNMT (1:1000) (24) in phosphate-buffered saline containing 0.1% Triton X-100. Coons' immunofluorescence method was used for detection (25). Dark-field photomicrographs of TH-IR fibers in striatum of a (C) nongrafted and (D) grafted (4 weeks after grafting) MPTP-treated mouse. The nongrafted striatum is at the same level as (D). Note absence of TH-IR in graft (G) and dense TH-IR fibers (white) surrounding graft. Mice were treated with two injections of MPTP at 50 mg per kilogram of body weight given 16 hours apart and were grafted 1 week later as described in the text. Sections were prepared as described in (B). TH-IR was detected with a biotin-avidin label (Vector Labs). Magnification, $\times 75$.

REFERENCES AND NOTES

1. C. C. Davis *et al.*, *Psychiatry Res.* **1**, 249 (1979).
2. J. W. Langston, P. Ballard, J. W. Tetrud, I. Irwin, *Science* **219**, 979 (1983).
3. R. S. Burns *et al.*, *Proc. Natl. Acad. Sci. U.S.A.* **80**, 4546 (1983).
4. P. Jenner, *Neurosci. Lett.* **50**, 85 (1984).
5. D. E. Redmond *et al.*, *Lancet* **1986-I**, 1125 (1986).
6. R. E. Heikkilä, A. Hess, R. C. Duvoisin, *Science* **224**, 1451 (1984).
7. H. Hallman, J. Lange, L. Olson, I. Stromberg, G. Jonsson, *J. Neurochem.* **44**, 117 (1985).
8. R. Fuller, D. W. Robertson, S. K. Hemrick-Luecke, *Biochem. Pharmacol.* **35**, 143 (1986).
9. S. J. Peroutka *et al.*, *Res. Commun. Chem. Pathol. Pharmacol.* **48**, 163 (1985).
10. L. R. Hegstrand and B. Eichelman, *Altex Chromatogram* **3**, 1 (1979).
11. M. F. D. Nottter, D. M. Gash, C. D. Sladek, S. L. Scharoun, *Brain Res. Bull.* **12**, 307 (1984).
12. C. C. Chiueh *et al.*, *Psychopharmacol. Bull.* **20**, 548 (1984).
13. H. Hallman, L. Olson, G. Jonsson, *Eur. J. Pharmacol.* **97**, 133 (1984).
14. J. P. Kessler, M. Nieto-Sampedro, J. Globus, C. W. Cotman, *Exp. Neurol.* **92**, 377 (1986).
15. A. J. Aguayo, A. Bjorklund, U. Stenevi, T. Carlstedt, *Neurosci. Lett.* **45**, 53 (1984).
16. Y.-A. Barde, D. Edgar, H. Thoenen, *Annu. Rev. Physiol.* **45**, 601 (1983).
17. J. M. Rosenstein and M. W. Brightman, *J. Comp. Neurol.* **250**, 339 (1986).
18. I. Irwin and J. W. Langston, *Life Sci.* **36**, 207 (1985).
19. A. J. Bradbury *et al.*, *Nature (London)* **319**, 56 (1986).
20. N. Tulipan, S. Huang, W. O. Whetsell, G. S. Allen, *Brain Res.* **377**, 163 (1986).
21. B. S. Bregman and P. J. Reier, *J. Comp. Neurol.* **244**, 86 (1986).
22. E.-O. Backlund *et al.*, in *Neural Grafting in the*

- Mammalian CNS*, A. Bjorklund and U. Stenevi, Eds. (Elsevier, Amsterdam, 1985), pp. 551–558.
23. I. Madrazo *et al.*, *N. Engl. J. Med.* **316**, 831 (1987).
24. M. C. Bohn, C. D. Dreyfus, W. Friedman, K. A. Markey, *Dev. Brain Res.*, in press.
25. A. H. Coons, in *General Cytochemical Methods*, J. F.

- Danielli, Ed. (Academic Press, New York, 1968), pp. 399–442.
26. We thank D. Sadri for expert technical assistance, M. Gupta for help in the early phases of this work, and D. Godden for help in preparing the manuscript. Supported by grants from the National Institutes of

Health (NS20832), a Research Career Development Award to M.C.B. (NS00910), a Jacob Javits Award to D.M.G. (NS15109), and a grant from the Familial Dysautonomia Foundation.

13 March 1987; accepted 11 June 1987

The Maize Transposable Element *Ds* Is Spliced from RNA

SUSAN R. WESSLER,* GEORGE BARAN,† MARGUERITE VARAGONA

In some instances, insertion of maize transposable elements into exons does not result in the total loss of enzymatic activity. In other instances, messenger RNAs of wild-type size are encoded by genes known to contain the maize transposable element *Dissociation* (*Ds*) in exons. To understand how *Ds* is processed from RNA, a study was made of transcripts encoded by two alleles of the maize *waxy* (*wx*) gene containing *Ds* insertions in exon sequences. The analysis was carried out in strains where the *Ds* element could not excise from the *wx* gene. Despite insertions of 4.3- and 1.5- *Ds* elements, the predominant transcripts encoded by these two genes were wild type in size. For both alleles, DNA sequencing of complementary DNAs revealed that the *Ds* elements had been spliced in a similar manner. Splicing was accomplished by the utilization of multiple 5' donor splice sites in the *Ds* termini and a 3' acceptor site within the *wx* gene adjacent to the *Ds* element. The net effect in both cases was the removal of most of the *Ds* element from the messenger RNA.

THE EXPRESSION OF GENES CONTAINING *Ds* (*Dissociation*) insertions can be analyzed either in the presence or absence of the *Ac* (*Activator*) element. Recent analyses of these elements have focused on gene expression in the presence of *Ac*, that is, when the *Ds* element can transpose. These studies have revealed how the excision of *Ds* can alter gene expression by adding nucleotides to a gene at the site of excision (1–5). In the present study, we analyzed the influence of *Ds* insertion on RNA transcripts in the absence of *Ac*; that is, when *Ds* cannot excise from the gene in which it is inserted. This study was prompted by two findings: (i) *Wx* (*waxy*) protein of wild-type size is produced in a strain containing a *wx* allele with a 4.3-kb *Ds* element in one of the exons (6), and (ii) two alleles of the *adh1* locus produce wild-type sized *Adh1* messenger RNAs (mRNAs) despite *Ds* insertions in exons (7, 8). To determine the sequences involved in the removal of *Ds* sequences from the primary transcripts, we characterized the RNAs produced by two alleles of the *wx* locus that have *Ds* insertions in two distinct exons.

The *wx* gene encodes a starch granule-bound enzyme responsible for the synthesis of amylose in endosperm tissue. The gene has been cloned (9) and sequenced (10) and the position and effect of several *Ac* and *Ds* insertions have been described (4, 11, 12). The positions of two *Ds* elements within the *wx* gene are displayed in Fig. 1B. The

cloning (11) and sequencing (13) of the *Ds* insertion in the *wx-m9* allele has also been described. Despite insertion of a 4.3-kb *Ds* element, endosperms harboring the *wx-m9* allele have significant amylose and produce reduced amounts of a wild-type sized *Wx* protein (6). In contrast to *wx-m9*, endosperms harboring the *wxB4* allele contain no amylose and have no *Wx* enzymatic activity (14).

Steady-state transcripts produced by these two *wx* alleles were analyzed by Northern blots (Fig. 2). Surprisingly, we found that in both cases the predominant *Wx* transcript is approximately 2.4 kb, the same size as the wild-type transcript. Rehybridization of the *wx-m9* blot with a *Ds*-specific probe indicated that the 2.4-kb transcript had no detectable homology with *Ds* but the minor transcripts of 6.7 kb and 1.8 kb were homologous with both *Ds* and *Wx* sequences (Fig. 2A). These data led us to conclude that the 6.7-kb transcript is a pre-mRNA that includes *Wx* mRNA (2.4 kb) and the entire *Ds* element (4.3 kb) while the 2.4-kb transcript arises following the processing of *Ds* from pre-mRNA. The 1.8-kb transcript is not homologous with *Wx* sequences downstream from the 3' site of *Ds* insertion and may represent a transcript that terminates within the *Ds* element. The precise nature of this small transcript has not been investigated further.

The relative abundance of the 2.4-kb transcripts in the *wx-m9* and *wxB4* strains sug-

gested that the *Ds* elements were efficiently spliced from *Wx* mRNA. To determine how these processed transcripts arose, we used samples of the RNA analyzed by Northern blots (Fig. 2) as templates for complementary DNA (cDNA) synthesis. Double-stranded cDNAs were inserted into λ gt10 and plaques screened with *Wx* specific probes. Recombinant phage DNAs that hybridized with *Wx* probes were subcloned and the DNA near the site of *Ds* insertion was sequenced (Fig. 1, A and D).

In addition to cDNA, genomic DNA containing the *wxB4* *Ds* insertion was also cloned and DNAs containing the *Ds* terminal and adjacent *Wx* sequences were subcloned and sequenced (Fig. 1C). We found that the *wxB4* *Ds* insertion is 1.5 kb and the termini have 316 and 257 bp, respectively, homologous with the *Ac* termini. The central 900 bp of this *Ds* element is not homologous with *Ac* (15). Pohlman *et al.* (13) previously determined that the 4369-bp *Ds* element in the *wx-m9* allele was derived from the 4563-bp *Ac* element by a 194-bp internal deletion.

The sequences compared in Fig. 3A reveal splicing sites (16) that would result in removal of most of the *Ds* element during RNA processing. Of the eight cDNAs analyzed, three had the sequence of cDNA I while five were like cDNA II (see the legend to Fig. 1D). The two cDNAs differ by the choice of 5' donor sites located only 4 bp apart. The splice acceptor site for both cDNAs is the same and is part of the 8-bp direct repeat of *Wx* sequences that is generated upon *Ds* insertion and flanks the element (Fig. 3). DNA sequencing also revealed that both cDNAs I and II utilize the same poly(A) addition site and that this site is one of three utilized in nonmutant *Wx* strains (10).

The cDNA I differs from wild-type *Wx* cDNA by the addition of 23 bp: 24 bp added from the 5' *Ds* terminus and 1 bp deleted from *Wx* sequences on the 3' end of the intron. The 8-bp direct repeat is also deleted but it was added to the *Wx* sequences upon insertion of *Ds* and one copy

Botany Department, University of Georgia, Athens, GA 30602.

*To whom correspondence should be addressed.

†Present address: Molecular Genetics Inc., 10320 Bren Road East, Minnetonka, MN 55343.